Section A -Research paper
ISSN 2063-5346

Evaluating the Microstructural Characteristics of Dissimilar AL Alloys Using FSW

Mohamad ummar
Email: mohamadummar786@gmail.com

Dr. Sachin saini
Email: sachin.saini@rimt.ac.in

Er. Ajay Rana
Email: ajayrana.me@rimt.ac.in

Abstract*—The optimization of process parameters of Friction stir welding have not gone in to the details of microstructural changes with variations in the parameters. The single consumable in the FSW process is the tool. The reported studies for the optimization of parameters for obtaining better results often suggested complex shape features for the tool which obviously increases the process cost. Gathering a suitable combination of process parameters with simple tool geometry, hence would have contributed much to the research in the area of FSW process. The thesis elucidates the experimental efforts to propose an optimum combination of parameters with simple tool geometry for FSW at higher linear speeds. Two precipitation hardenable aluminium alloys were selected as the materials for study: AA2024 and AA6061. Both are light weight and possess high strength to iv weight ratio. AA2024 alloy is popular in the aviation manufacturing and AA6061 is a pioneer material in the structural applications. For the precipitation hardened alloys the concentration and distribution of the strengthening precipitates is most influential for the strength of the alloys. Hence the distribution and dissolution of the strengthening particles under the influence of the process parameters are crucial in the study of friction stir welds. Taguchi analysis which is very useful for the identification of the control factors to obtain optimum results for the process was used to design the experiments and further analysis. The effect of process parameters on the microstructural changes in the weld region and on the defect formation was also investigated. The experiments were conducted with, perhaps the highest welding speed reported, so far. Through the analysis, optimum combinations of the parameters were suggested for each material at a high speed friction stir window. An analytical model was proposed from the basic theory and parameters for suggesting the process parameters and tool parameters for various aluminium alloys. The computed results of the model were validated by comparing with the reported results.

I. INTRODUCTION

A. *Welding*

Welding is the metal joining process or fabrication process in which heat and pressure are involved in the making of a permanent joint between two materials involved in the joining process. The materials are heated to a high temperature at the edges and after reaching softening point or melting; the edges of two materials are brought together and joined by applying pressure or without that. Welding is different from the brazing and soldering processes that involve low temperature heating and are suitable to join very thin materials.

Welding originated in Europe and Middle East during the Bronze and Iron ages. In ancient Greece, people used the welding technology for making iron pillars. Blacksmiths contributed thus most of the part in forge welding where they heated the material for softening and joined them together to form a new joint. The arc welding practiced during the eighteenth century was popular among the materials scientists and industrialists.

During the nineteenth century, resistance welding and thermit welding were developed and used by people for joining materials through creation of electrical resistance and for producing heat at the edges of the materials and making perfect permanent weld joints. The growth of welding reached a huge milestone during the World War I when the arc welding method was used in the fabrication of ships and aircrafts. The British used the arc welding technique in the fabrication of most of their military weapons, tanks,marine equipments and aero applications. During the 1920s, major improvements were made in the arc welding process through introduction of flux and automatic movement of electrode with respect to a work piece that prevented the formation of porosity in the weld region and the brittleness of the weld materials.

II. MATERIALS AND METHODS

A. *MATERIALS*

Aluminum alloys AA2024 and AA6061 can retain strength in environments like marine and Petro-chemical industries against chemical and corrosion attack. Hence, they are the choice of material scientists and industrialists in marine applications. In this research work, AA2024 and AA6061 were used for the fabrication of dissimilar weld joint using friction stir welding. The aluminum alloy material AA5083- H111 contains magnesium, manganese and chromium as major elements and is used in the chemical and marine applications. The aluminum alloy AA6061-T6 possesses better mechanical and weldability characteristics. The properties of parent materials AA2024 and AA6061 are given in Table 1 and chemical composition of the AA2024 and AA6061 is shown in Table 2.

(Source: Data sheet of Aalco Metals Ltd.Wednesbury, UK)

(Source: Data sheet of Aalco Metals Ltd.Wednesbury, UK)

1) FRICTION STIR WELDING: Friction stir welding (FSW) is performed in solid state that uses non-consumable tool to join the work pieces together. Initially, the tool is rotated at pre-determined speed and traversed along the joining line of the work piece. Rotation of the tool generates heat and softens the edges of the work pieces near the joining line.

TABLE I
PHYSICAL AND MECHANICAL PROPERTIES OF AA2024 AND AA6061 ALLOYS

Sl. No.	Property	AA2024	AA6061-T6
1	Density	2650 kg/m^3	2700 kg/m^3
2	Melting Point	570 ˚C	650 ˚C
3	Modulus of Elasticity	72 GPa	70 GPa
4	Electrical Resistivity	0.058x10^{-6} Ω. m	0.040 x10^{-6} Ω. m
5	Thermal Conductivity	121 W/m. K	166 W/m. K
6	Thermal Expansion	25x10^{-6} /K	23.4 x10^{-6} /K
7	Ultimate Tensile Strength	317 MPa	310 MPa
8	Yield strength	228 MPa	276 MPa
9	Elongation (%)	16	12
10	Hardness Brinell	75 HB	95 HB

TABLE II
TABLE 2 CHEMICAL COMPOSITION OF PARENT MATERIALS

Aluminum alloy	Chemical compositions (wt %) Si	Fe	Cu	Mn	Mg	Cr	Zn	Ti	Al
6061-T6	0.4-0.8	0.7 Max	0.15-0.4	0.15 Max	0.8-1.2	0.04-0.35	0.25 Max	0.15Max	Bal
5083-H111	0.4 Max	0.4 Max	0.10 Max	0.4 - 1.0	4.0-4.9	0.05-0.25	0.10 Max	0.05-0.25	Bal

The softened edges are forged by tool pressure and a solid-state welding is made. The process of friction stir welding is shown in Figure 1 and a photograph of friction stir welding machine is shown in Figure 2. The specifications of the FSW machine are shown in Table 3 (a).

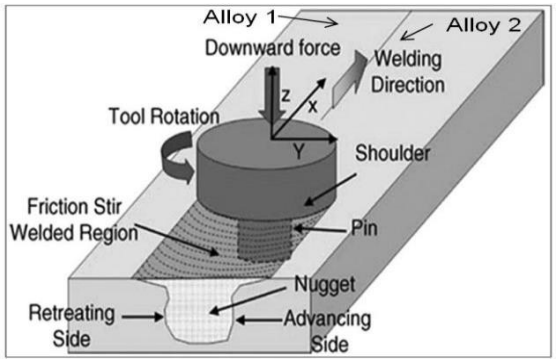

Fig. 1. Friction stir welding arrangement **(Source: Sundaravel Vijayan et al. 2010)**

A single pass butt welding joint was made using 6 mm thickness plates of AA2024 and AA6061, the process parameters used are detailed in Table 4. The work piece dimensions were 200 mm ✖100 mm ✖6 mm and the tool used was made up of H13 steel material. While performing the welding, the aluminum alloy AA2024 was used in the advancing side and AA6061-T6 was placed in the reversing side and the tool was

Fig. 2. **FSW sample at rotational speed of 800 rpm and cylindrical tool pin**

traversed along the 200 mm side of the work piece (Durga prasad et. al 2016). Figure 3 to 5 show the different tool pin shapes used in the FSW process. The welded work piece sample at a rotational speed of 800 rpm with cylindrical pin tool is shown in Figure 6.

B. SEM ANALYSIS

The specimens for the scanning electron microscope were cut perpendicular to the welding direction by means of the wire cut electrical discharge machine (EDM) of High tech make and model number DK7725 and is shown in Figure 3.7. The EDM is a multi-cut type capable upto 7 passes with a 0.18 mm molybdenum wire. All the weld samples were polished using a grit sequence of 220, 320, 500, 800 and 1200. After polishing the surfaces to be examined in the welded samples, they were etched with Dix-Keller reagent. Morphological changes in the microstructure were observed and recorded for 1000x using the TESCAN scanning electron microscope (SEM) of model VEGA3 which is shown in Figure 3.8. The machine has a magnification capability of 500x to 5000x and an acceleration voltage range of 10-20 kV.

C. TENSILE STRENGTH ANALYSIS

Tensile strength is the ability of the material to withstand the axial loading or axial pulling that determines the suitability of the materials in various engineering applications. Tensile strength is the property of the material that does not depend on the size of the material. Hence, the specimen size does

ISSN 2063-5346

TABLE III
(A) SPECIFICATIONS OF FSW MACHINE

S. No.	Particu-lars	Specification
1	Work table size	The maximum length of 800mm and width of 400mm provided with standard t-slots, maximum table tilt 45˚ on either side concerning the spindle axis.
2	Provision for tilting the tool X axis	Tool head ± 3^{O} tilt with easy adjustable feature.
3	Drive system	Servo motor with servo gear box
	Stroke	600 mm
	Feed	0 – 1500 mm/min (indefinitely variable).
	Thrust force Y-axis	250 Kgf(min) – 2500 Kgf (max) hydraulic pressure.
4	Drive system	Servo motor with servo gear box
	Stroke Z axis	250mm
5	Drive system	Servo motor with servo gear box
	Stroke	325mm
	Speed	Rapid traverse for positioning - 2000 mm/min
	Force	500 Kgf (min) to 3000 Kgf (min)
6	Spindle speed	50 - 2750rpm
7	Spindle motor	12 - 15 KW / 440V (AC Drive)
8	Tool holder	To be matched with Spindle bore, i. e., ISO40 & ER40
9	Collet	Outer diameter to be matched with the tool holder and inner diameter holding size of an 18 to 25mm.
10	Lubrica-tion	Centralized Lubrication system controlled by PLC.

TABLE IV
FSW PARAMETERS

S. Nc	Parameter	Description
1	Material	AA2024 &AA6061-T6
2	Traverse Speed	44,72 and 100 mm/min
3	Piercing Depth	5.3 mm
4	Rotational Speed	800, 1000 and 1200 rpm
5	Tool Pin Profile	Cylindrical, tapered & threaded

Fig. 3. Wire cut electrical discharge machine

Fig. 4. **TESCAN scanning electron microscope**

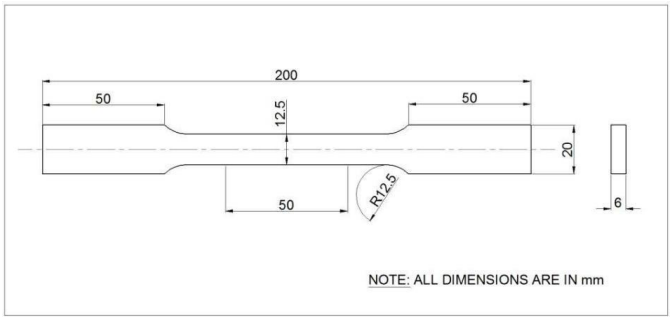

Fig. 5. Tensile test specimen

not have any influence on the tensile strength. However, the standard size of the specimen was followed here in the performance of the tensile test according to the ASTM standards as displayed in Figure 5 In this investigation, the tensile test was conducted on the Universal Testing Machine of FIE make and model name of UTN-10 which is shown in Figure6. The capacity of the machine is 10 tons and is driven by a hydraulic power pack. The machine has a ram stroke of 150 mm and a maximum working clearance of 700 mm. Tensile tests were conducted for the materials AA2024 and AA6061 and friction stir welded joints of AA5083- H111 – AA6061-T6 as per ASTM-E8 standard.

D. Taguchi L-27 TECHNIQUE

Design of Experiments (DoE) is the common procedure used for a reduction in the time and cost of the experimental

ISSN 2063-5346

Fig. 6. **Universal Testing Machine**

work. Taguchi L-27 technique is one of the DoE procedures for finding the optimal parameters that influence the output of the experimental work. It is the statistical tool applied for many problems in industrial applications. Taguchi L-27 procedure finds the most influencing parameter with less expenditure and time consumption. The selection of parameters is optimal in the design of experiments and the forecasting of the output is quite simple and economical to use in the real applications (Rao et al. 2008). Taguchi L-27 procedure illustrated in Figure 3.19 involves designing of the experiment using the orthogonal array approach. The experiments are further conducted for a set of experiments with the combination of the parameter levels as arrived in the orthogonal array. The optimal levels of the parameters arrived at were based on the criteria specified and verified with the confirmation experiment. Once the outcome of the confirmation experiment is comparable with the expected outcome, the parameter levels are declared as optimum levels. Otherwise, the orthogonal array is further refined to get more reliable results.

III. EXPERIMENT AND ANALYSIS

Analysis of Hardness and Tensile Strength Friction stir welding was performed for the joining of dissimilar aluminum alloy materials AA2024 and AA6061 to analyze the ability of the material to withstand severe environmental conditions of sub-sea applications. Prior to the erosion – corrosion test, the friction stir welded joints were analyzed for the optimal joint strength. Initial samples during establishing the process were cut and the cross section were inspected for defects and qualified. The welded samples were checked visually after welding.

Micro hardness and tensile tests were carried out at the weld centre of specimen fabricated by varying the rotational speed from 800 rpm to 1200rpm, traverse speed from 44 mm/min to 100 mm/min and at different tool pin profiles. All the experimental readings of hardness and tensile strength analysis of the material were interpreted and the results are tabulated in the Table 5.

, shows that the weld specimen prepared by the cylindrical tool pin profile at 800 rpm rotational speed and 44 mm/min

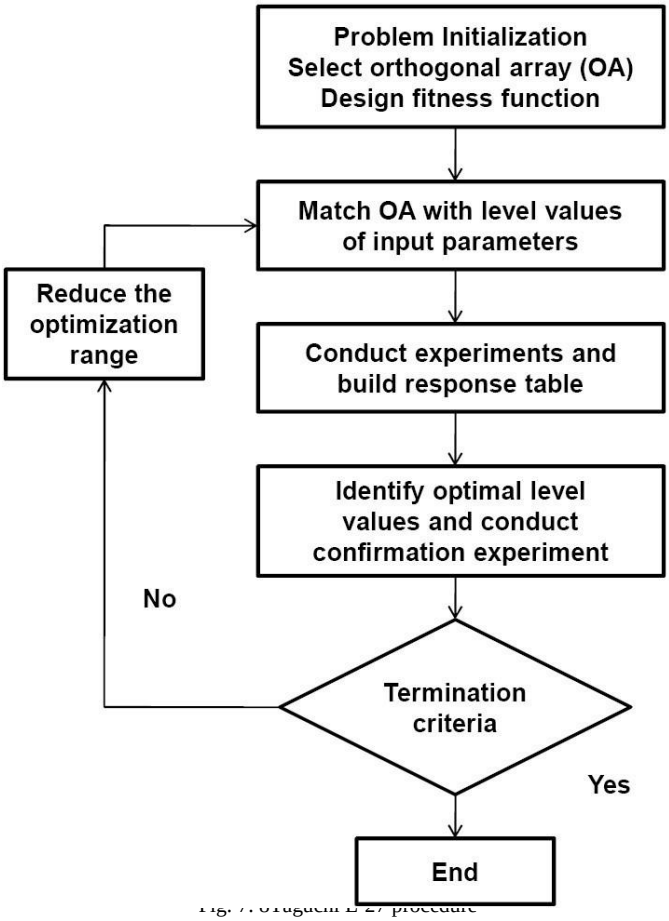

Fig. 7. Taguchi L-27 procedure

TABLE V
HARDNESS AND TENSILE STRENGTH RESULTS

Ex. No	Input Parameters			Breaking Load (kN)	Hardness (Hv)
	Rotational Speed (rpm)	Traverse speed (mm/min)	Tool pin shape		
1	800	44	Cylindrical	5.83	76.5
2	800	72	Threaded	5.07	78.86
3	800	100	Tapered	3.61	84.96
4	1000	44	Threaded	5.15	74.56
5	1000	72	Tapered	3.38	79.9
6	1000	100	Cylindrical	4.25	77.15
7	1200	44	Tapered	3.05	74.5
8	1200	72	Cylindrical	4.20	72.93
9	1200	100	Threaded	4.12	74.55

welding traverse speed having the maximum breaking load of 5.83 kN. A maximum hardness value of 84.96 Hv was observed for the weld specimen fabricated by taper pin profile at 800 rpm rotational speed and 100 mm/min traverse speed. Hence, the cylindrical tool profile having a shoulder diameter of 15 mm and a pin diameter of 6 mm was selected. In friction stir welding, due to tool rotation, distortions may result in the nearby region and due to the shear flow of material and the grains may get elongated.The weld centre experienced high temperature while per- forming friction stir welding and underwent severe plastic deformation that modified the large grain size into fine grain. Further, the microstructure grain shape was observed as equi- axed and equally spaced that resulted in superior strength and hardness at the weld centre compared to other regions.

1) Micrographic Characterization: Micro structural analysis was carried out using the Scanning Electron Microscope (SEM) and Energy Dispersion Spectrum (EDS) and the material characteristics were explored for the specimen of base alloys and the weld zone of the dissimilar welded joint which possessed the maximum tensile strength, obtained with a rotational speed of 800 rpm, traverse speed of 44 mm/ min and with cylindrical pin tool. The dimensions of the cylindrical pin tool are shown in Figure 4.1.

Figure 9(a) shows the SEM image of the AA2024 aluminum alloy material and Figure 10(b) shows the SEM image of the aluminum alloy AA6061-T6. As can be seen from the SEM images, the microstructure of

AA2024 displayed elongated grains and the microstructure of A6061 revealed uniformity in grain structure. Microstructures of both AA2024 and AA6061 aluminum alloy showed no impurities throughout the structure. Figure 11(c) shows the SEM image taken at near welded region of AA2024 aluminum alloy and Figure 4.2(d) shows the SEM image taken at near welded region of the AA6061-T6 aluminum alloy.

The grain arrangement in the welded region near AA2024 shown in Figure 11(c) is well and equiaxed and the grain size is significantly lesser than that in the base material (AA2024) due to the much higher temperature and extensive plastic deformation by the stirring action of the tool. During FSW, the tool basically acts as a stirrer which extrudes the material in the direction of the welding. The recrystallization process which results in finer grain size, highly depends on the rate of cooling and the temperature generated during welding.

Aluminium alloy AA6061-T6 is highly sensitive to flow and softening at high temperature, and easily forms a plastic deformation, while AA2024 is steady in softening at high temperature. Aluminium alloy AA6061-T6 is easily moved by tool and has good weld ability during FSW while compared to AA2024 . The welded region near AA6061-T6 in the heat affected zone is shown in Figure 12(d) shows large grains and equal spacing.While performing the friction stir welding, the heat gener- ated around the welded region also created a plastic deformation and developed the fine grain of microstructure in the areas adjacent to the weld zone. Figure 4.2(e) shows the SEM image of the weld centre. The image clearly shows the weld centre pointing to two distinct regions such as the Heat Affected Zone (HAZ) and the Stir Zone (SZ). SZ is the main zone of welded area that experiences more heat generation during the welding process and thus goes through severe plastic deformation of microstructure, thereby achieving strength superior to the other zone. The SZ is characterized by deformed, elongated grains reflecting the direction of material flow in the welding process. Deformation of SZ structure is the result of high stress and large deformation occurring due to the mechanical force of the rotating pin. At the same time, a far more homogeneous microstructure characterized by fine grains is achieved at SZ.

HAZ is the zone nearer to SZ that was also affected by the heat generated during the welding process. However, the effect of heat was not severe as that of SZ, hence the plastic deformation observed was less. Hence modification seen in the grain size was less compared to that of changes observed in the microstructure of the SZ. The boundary between HAZ and SZ can be clearly observed in Figure 13 (e).

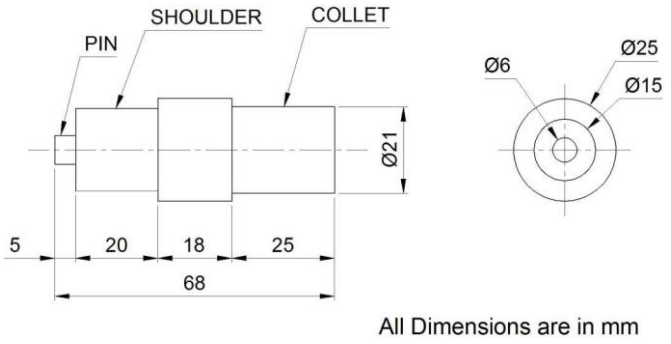

Fig. 8. Cylindrical pin tool drawing

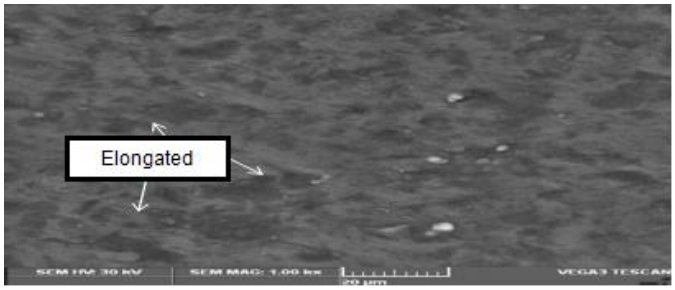

Fig. 9. **a)SEM image of AA2024**

Energy Dispersive X-ray Spectroscopy (EDS) study is used for getting an understanding of the metal elements present in the materials and to analyze the materials property based on the metallic elements. The EDS results of dissimilar material AA2024 – AA6061-T6 taken at the weld interface are shown in Figure 4.3. As can be seen from the Figure 4.3, the Al element is displayed in a large amount and magnesium, zinc and chromium are exhibited in an intermediate amount. At the

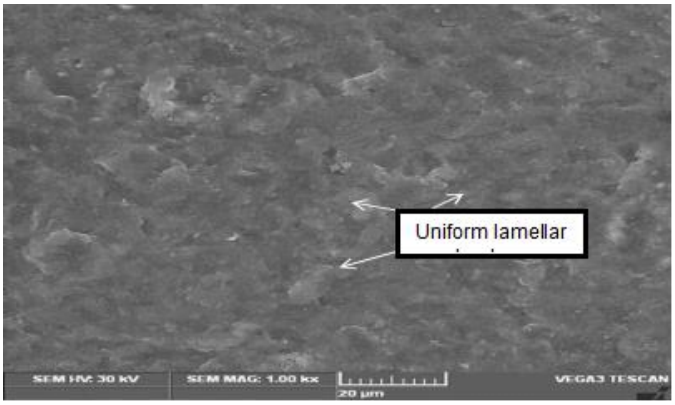

Fig. 10. b) SEM image of AA6061-T6

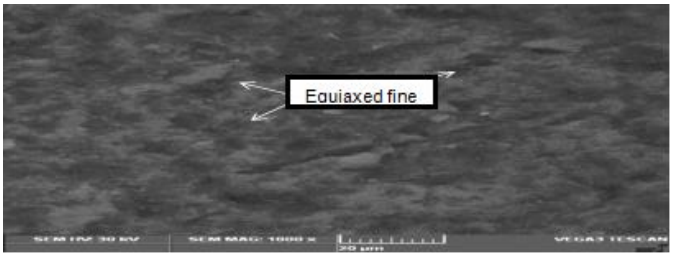

Fig. 11. c) **SEM Image of welded region near AA2024**

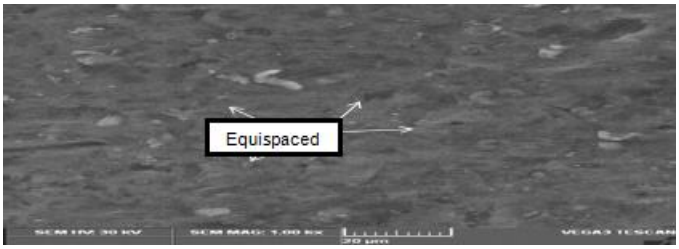

Fig. 12. d) SEM Image of welded region near AA6061-T6

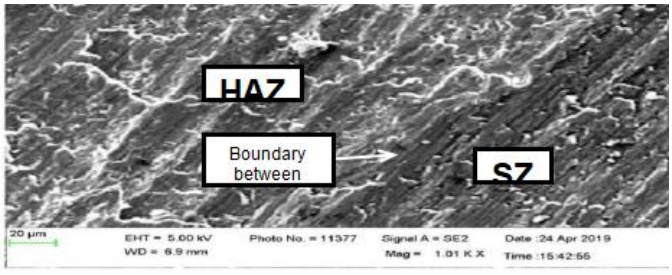

Fig. 13. e) **SEM Image taken at weld centre**

weld interface, magnesium was observed as the major element than zinc and titanium since magnesium is the chief alloying element of AA2024 . The presence of larger amounts of magnesium elements in the welded joint could have contributed to the lower fatigue strength of AA2024 – AA6061-T6 dissimilar joint materials.

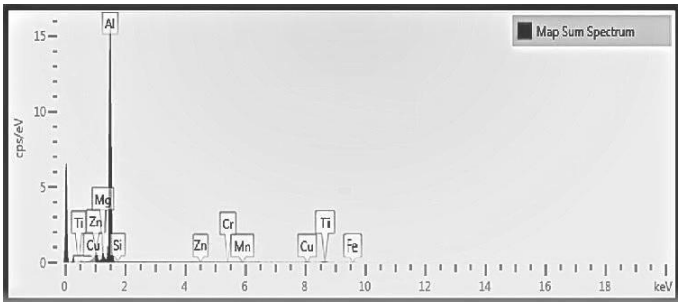

Fig. 14. e 4.3 EDS analysis of AA2024 -AA6061-T6 weld joint

B. EROSION-CORROSION ANALYSIS

Erosion – corrosion is the mechanical deterioration in the material surface caused by the combined action of erosion and corrosion by abrasive slurry, particles suspended in the liquid or gas medium and impingement of the liquid. Material removal is initially accelerated by mechanical erosion and then the corrosive action is accelerated until the perforations of the material occur. Erosion – corrosion analysis is used for the determination of the material strength for the specific applications like marine, aero and sub-sea engineering. In this research work, the erosion – corrosion analysis was performed on the specimens of AA2024 , AA6061-T6 and friction stir welded joints of aluminum alloys AA2024 and AA6061 for testing the suitability of the material for sub-sea applications. The detailed discussion about the erosion – corrosion analysis of the aforementioned test material is presented in this section.

IV. CONCLUSION

FSW is a formidable development in material joining process. It is considered as a better option for joining aluminium alloys. In this scenario, two extreme cases can be considered; precipitation hardened alloys and solid solution hardened alloys. Both these are weldable by conventional fusion welding processes. However, precipitation hardened alloy welds were found to be more defective under fusion welding. Hence FSW is a promising technology for these types of aluminium alloys. In this work FSW of precipitation hardened alloys were dealt with by considering **AA2024 (Al-Mg alloy) and AA6061-T6(Al-Mg-Si)** alloys as representative examples. The effect of various parameters on the strength and microstructure were analysed. The parameters were so chosen that they can be easily adjusted in the dedicated machines presently available. Simple tool geometries with tapered, cylindrical and threaded pin profiles were selected so as to minimize the initial cost. The welding is performed at higher linear speeds to enhance the productivity. Hence the experimental analysis

focused on the commercialization and popularisation of the technology. Effect of axial force on the FSW was explored taking AA 6082 – T6 as the base metal. Experiments were conducted by varying the axial force when other parameters were kept constant. Process parameters considered were tool rotational speed and tool translational or linear speed with a threaded pin profile. Even for these parameters selected form a 'process window' for good weld conditions as recommended by previous studies, axial force was found to influence the weld properties significantly.

REFERENCES

[1] Muruganandan and Das, "Friction stir welding process parameters for joining dissimilar aluminium alloys," *International Journal of Mechanical engineering and Technology*, vol. 2, no. 2, pp. 25–38, 2011.
[2] K. Surekha, B. S. Murthy, and K. R. Prasad, "Microstructural characterization and corrosion behaviour of multipass friction stir processed AA 2219 aluminium alloy," *Surface & Coating Technology*, vol. 202, pp. 4057–4068, 2008.
[3] C. Dawes and W. M. Thomas, "Friction Stir Process Welds Aluminium Alloys," *Welding Journal*, vol. 75, pp. 41–45, 1996.
[4] H. Fujii, L. Cui, M. Maeda, and K. Nogi, "Effect of tool shape on mechanical properties and microstructure of friction stir welded aluminium alloys," *Journal of Materials Science and Engineering A*, vol. 419, pp. 25–31, 2006.
[5] Y. Chao and X. Qi, "Thermal and thermo-mechanical modelling of friction stir welding of aluminium alloy 6061 - T6," *Journal of Material Processing and Manufacturing Science*, vol. 7, pp. 215–233, 1998.
[6] M. Z. H. Khandkar, J. A. Khan, and A. P. Reynolds, "Prediction of temperature distribution and thermal history during friction stir welding: input torque model," *Science and Technology of Welding and Joining*, vol. 8, pp. 165–174, 2003.
[7] R. Palanivel and P. K. Mathews, "Prediction and optimization of process parameter of friction stir welded AA5083-H111 aluminum alloy using response surface methodology," *Journal of central south university*, 2012.
[8] W. M. Thomas, E. D. Nicholas, J. C. Needham, M. G. Murch, P. Temple-Smith, and C. J. Dawes, 1991.
[9] R. M. Mishra and M. W.
[10] R. Mishra and Z. Ma, 2005.
[11] R. Rai, A. De, H. K. D. H. Bhadeshia, and T. Debroy, pp. 325–342, 2011.
[12] P. Cavaliere, G. Campanile, F. Panella, and A. Squillace, "Effect of welding parameters on mechanical and microstructural properties of AA6056 joints produced by friction stir welding," *Journal of Materials Processing Technology*, vol. 180, pp. 263–270, 2006.
[13] V. Firouzdor and S. Kou, "Al-to-Mg friction stir welding: effect of material position, travel speed and rotation speed," *Metallurgical and Materials Transactions A*, vol. 41, pp. 2914–2935, 2010.
[14] P. Colegrove, M. Painter, D. Graham, and T. Miller, "-dimensional flow and thermal modelling of the friction stir welding process proceedings of second international symposium on friction stir welding," 2000, pp. 3–3.
[15] S. W. Kallee, J. Davenport, and E. D. Nicholas, "Railway Manufacturers implement friction Stir Welding," *Welding Journal*, vol. 81, pp. 47–50, 2002.
[16] P. Cavaliere, D. A. Santis, F. Panella, and A. Squillace, "Effect of anisotropy on fatigue properties of 2198 Al - Li plates joined by friction stir welding," *Engineering Failure Analysis*, vol. 6, pp. 1856–1865, 2008.
[17] S. Rajakumar, C. Muralidharan, and V. Balasubramanian, "Optimization of the friction stir welding process and tool parameters to attain a maximum tensile strength of AA7075-T6 aluminium alloy," *Proceedings of the Institution of Mechanical Engineers*, vol. 224, no. 8, pp. 1175–1191, 2010.
[18] W. Tang, X. Guo, J. C. Mcclure, L. E. Murr, and Nunes, "Heat Input and Temperature Distribution in Friction Stir Welding," *Journal of Materials Processing and Manufacturing Science*, vol. 7, no. 2, pp. 163–172, 1988.
[19] S. Malarvizhi and V. Balasubramanian, "Effect of welding processes on AA2219 aluminium alloy joint properties," *Transactions of Nonferrous Metals Society of China*, vol. 21, pp. 962–973, 2011.
[20] H. N. B. Schmidt, T. L. Dickerson, and J. H. Hattel, "Material flow in butt friction stir welds in AA2024-T3," *Acta Materialia*, vol. 54, pp. 1199–1209, 2006.
[21] M. Jayaraman and V. Balasubramanian, pp. 605–615, 2013.
[22] "An analytical model of heat generation for eccentric cylindrical pin in friction stir welding," *Journal of Materials Research and Technology*, vol. 5, no. 3, pp. 234–240, 2016.
[23] Z. Zhang, B. L. Xiao, and Z. Y. Ma, "Effect of welding parameters on microstructure and mechanical properties of friction stir welded 2219 Al- T6 joints," *Journal of Material science*, vol. 47, pp. 4075–4086, 2012.
[24] A. P. Reynolds, "Flow visualization and simulation in FSW," *Scripta Materealia*, vol. 58, pp. 338–342, 2008.
[25] M. Attallah, G. Hanadi, and Salem, "Friction stir welding parameters: a tool for controlling abnormal grain growth during subsequent heat treatment," *Materials Science and Engineering: A*, vol. 391, pp. 51–59, 2004.
[26] 2007.
[27] H. Schmidt, J. Hattel, and J. Wert, "An analytical model for the heat generation in friction stir welding. Modelling and Simulation of," *Materials Science and Engineering*, vol. 12, pp. 143–157, 2004.
[28] 2011.
[29] O. Hatamleh and A. Dewald, "An investigation of peening effects on the residual stresses in friction stir welded 2195 and 7075 aluminum alloy joints," *Journal of Materials Processing Technology*, vol. 209, pp. 4822–4829, 2009.
[30] J. Q. Su, T. W. Nelson, R. Mishra, and M. Mahoney, "Microstructural investigation of friction stir welded 7050- T651 aluminium," *Acta Materialia*, vol. 51, no. 3, pp. 713–729, 2003.
[31] H. Aydin, A. Bayram, A. Uguz, and S. K. Akay, "Tensile properties of friction stir welded joints of 2024 aluminum alloys in different heat treated- state," *Materials and Design*, vol. 30, pp. 2211–2221, 2009.
[32] M. Russell and H. R. Shercliff, *Analytical modelling of microstructure development in friction stir welding First International Symposium on Friction Stir Welding*, Thousand Oaks, 1999.
[33] C. Devanathan, A. Murugan, and A. Sureshbabu, "Optimization of process parameters in friction stir welding of Al 6063," *International Journal of Design and Manufacturing Technology*, vol. 4, no. 2, pp. 42–48, 2013.
[34] V. Gadakh and K. K. Adepu, "Heat generation model for taper cylindrical pin profile in FSW," *Journal of Materials Research and Technology*, vol. 2, no. 4, pp. 370–375, 2013.
[35] J. C. Mcclure, T. Tang, L. E. Murr, X. Guo, and Z. Feng, *A Thermal Model for Friction Stir Welding*, J. M. Vitek, S. A. David, and J., Eds.
[36] P. Podrzaj, P. Jerman, and D. Klobcar, "Welding defects at friction stir welding," *Metalurgija*, vol. 54, no. 2, pp. 387–389, 2015.
[37] V. Thomas and E. D. Nicholas, "Friction Stir Welding for the Transportation Industries," *Materials and Design*, vol. 18, pp. 269–273, 1997.
[38] W. Xu, J. Liu, G. Luan, and C. Dong, "Temperature evolution, microstructure and mechanical properties of friction stir welded thick 2219-O aluminium alloy joints," *Materials and Design*, vol. 30, pp. 3460–3467, 2008.
[39] S. Kanwar, S. Arora, M. Pandey, R. Schaper, and Kumar, pp. 941–952, 2010.
[40] M. Yu, E, and Z. Zhenqiang, "Structure response in the riveted and friction stir welded stringer panel under the tensile loading 13th international conference on fracture," 2013, pp. 16–21.
[41] H. Aydin, A. Bayram, and I. Durgun, "The effect of post- weld heat treatment on the mechanical properties of 2024- T4 friction stir- welded joints," *Materials and design*, vol. 31, pp. 2568–2577, 2010.
[42] . J. Yuh, X. Chao, W. Qi, and Tang, "Heat Transfer in Friction Stir Welding- Experimental and Numerical Studies," *Transactions of the ASME*, vol. 125, pp. 138–145, 2003.
[43] G. Oertelt, S. S. Babu, S. A. David, and E. A. Kenik, pp. 71–79, 2001.
[44] T. Seidel and A. P. Reynolds, "Visualization of the material flow in AA2195 friction-stir welds using a marker insert technique," *Metallurgical and Materials Transactions A*, vol. 32, pp. 2879–2884, 2001.
[45] Singh, S. G., and A. . Rana, " Experimental Investigation of the Friction Stir Welded Dissimilar Aluminium Alloys." *International Journal for Research in Applied Science & Engineering Technology*, vol. 10, no. IV, 2022.